WIDESPAN MEMBRANE ROOF STRUCTURES: DESIGN ASSISTED BY EXPERIMENTAL ANALYSIS

M. Majowiecki
IUAV
University of Venice, ITALY

Key words: wide span structures , snow and wind loading, experimental analysis, reliability.

Abstract. *Wide span structures are today widely applied for sport, social, industrial, ecological and other activities. The experience collected in last decades identified structural typologies as space structures, cable structures, membrane structures and new - under tension - efficient materials which combination deals with lightweight structural systems, as the state of art on long span structural design. In order to increase the reliability assessment of wide span structural systems a knowledge based synthetical conceptual design approach is recommended. Theoretical and experimental in scale analysis, combined with a monitoring control of the subsequent performance of the structural system, can calibrate mathematical modelling and evaluate long term sufficiency of design.*

1 INTRODUCTION:

Considering the statistical results of [1] , the unusual typologies, new materials and the “scale effect” of long span structures, several special design aspects arise as:

- the snow distribution and accumulations on large covering areas in function of statistically correlated wind direction and intensity;
- the wind pressure distribution on large areas considering theoretical and experimental correlated power spectral densities or time histories;
- rigid and aeroelastic response of large structures under the action of cross-correlated random wind action considering static, quasi-static and resonant contributions;
- the time dependent effect of coactive indirect actions as pre-stressing, short and long term creeping and temperature effects;
- the local and global structural instability;
- the non linear geometric and material behaviour;
- reliability and safety factors of new hi-tech composite materials;
- the necessity to avoid and short-circuit progressive collapse of the structural system due to local secondary structural element and detail accidental failure;
- the compatibility of internal and external restrains and detail design, with the modeling hypothesis and real structural system response;
- the parametric sensibility of the structural system depending on the type and degree of static indeterminacy and hybrid collaboration between hardening and softening behaviour of substructures.
- In the case of movable structures, the knowledge base concerns mainly the moving cranes and the related conceptual design process have to consider existing observations, tests and specifications regarding the behaviour of similar structural systems. In order to fill the gap, the IASS working group n°16 prepared a state of the art report on retractable roof structures [2] including recommendations for structural design based on observations of malfunction and failures.

From the observations of the in service performance, damages and collapses of all or part of structural systems, we have received many informations and teachings regarding the design and verification under the action of ultimate and serviceability limit states. Limit state violation for engineered structures have lead to spectacular collapses as the Tay (1879) and Tacoma bridges (1940). Sometimes an apparently "unimaginable" phenomenon occurs to cause structural failure. The Tacoma Narrows Bridge previously cited was apparently one such a case. It was also a design which departed considerably from earlier suspension bridge design.

Long span coverings were subjected to partial and global failures as that of the Hartford Colisseum (1978), the Pontiac Stadium (1982) and the Milan Sport Hall (1985) due to snow storms, the Montreal Olympic Stadium due to wind excitations of the membrane roof (1988), the Minnesota Metrodome (1983) air supported structure that deflated under water ponding, etc. Those cases are lessons to be learned from the structural failure mechanism in order to identify the design and construction uncertainties in reliability assessment. Many novel projects of long span structures attempt to extend the "state of the art". New forms of construction and design techniques generate phenomenological uncertainties about any aspect of the possible behavior of the structure under construction service and extreme conditions.

Fortunately, structures rarely fail in a serious manner, but when they do it is often due to causes not directly related to the predicted nominal loading or strength probability distributions. Other factors as

human error, negligence, poor workmanship or neglected loadings are most often involved (Ref 1). Uncertainties related to the design process are also identified in structural modelling which represents the ratio between the actual and the foreseen model's response.
According to Pugsley (1973), the main factors which may affect "proneness to structural accidents" are:

- new or unusual materials;
- new or unusual methods of construction;
- new or unusual types of structure;
- experience and organization of design and construction teams;
- research and development background;
- financial climate;
- industrial climate;
- political climate.

Cause	%
Inadequate appreciation of loading conditions or structural behaviour	43
Mistakes in drawings or calculations	7
Inadequate information in contract documents or instructions	4
Contravention of requirements in contract documents or instructions	9
Inadequate execution of erection procedure	13
Unforeseeable misuse, abuse and/or sabotage, catastrophe, deteriora tion (partly "unimaginable"?)	7
Random variations in loading, structure, materials, workmanship, etc.	10
Others	7

Table 1 Prime causes of failure. Adapted from Walker (1981).

All these factors fit very well in the field of long span structures involving oftenly something "unusual" and clearly have an influence affecting human interaction.
In Table 1, the prime cause of failure gives 43% probability (Walker, 1981) to inadequate appreciation of loading conditions or structural behaviour. Apart from ignorance and negligence, it is possible to observe that the underestimation of influence and insufficient knowledge are the most probable factors in observed failure cases (Matousek & Schneider, 1976).
Performance and serviceability limit states violation are also directly related to structural reliability. Expertise in structural detail design, which is normally considered as a micro task in conventional design, have an important role in special long span structures: reducing the model and physical uncertainties and avoiding chain failures of the structual system.

According to the author, knowledge and experience are the main human intervention factors to filter gross and statistical errors in the normal processes of design, documentation, construction and use of structures.
The reliability of the design process in the field of special structures must be checked in the following three principal phases: the conceptual design, analysis, and working design phases.

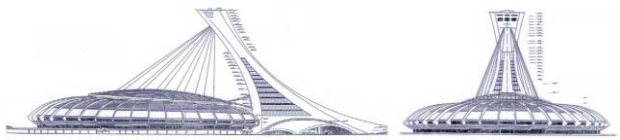

Figure 1 Montreal Olympic Stadium - A cable stayed roof solution

1.1 Some wide span enclosures

Long span structures needs special investigations concerning the actual live load distribution and intensity on large covering surfaces. Building codes normally are addressed only to small-medium scale projects. The uncertainties relate to the random distribution of live loads on long span structures imply very careful loading analysis using special experimental analysis.

Due to the lack of space, only some design&analysis illustrations of wide span enclosures, where the author was directly involved, will be included in the present paper with the intention to transmit some experiences that today may be part of the knowledge base.
From the direct author's experience in designing large coverings, the most important experimental investigation regarding live load distribution concerns the snow drift and accumulation factors and the dynamic action of wind loading.

2 DESIGN ASSISTED BY EXPERIMENTAL ANALYSIS

2.1 Snow loading experimental analysis on scale models

Olympic Stadium in Montreal. During the design of the new roof for the Montreal Olympic Stadium (Figure 1) a special analysis of snow loading was made considering three roof geometries varying the sag of the roof from 10 m, 11.5 m and 13 m.,in order to find a minimization of snow accumulation.

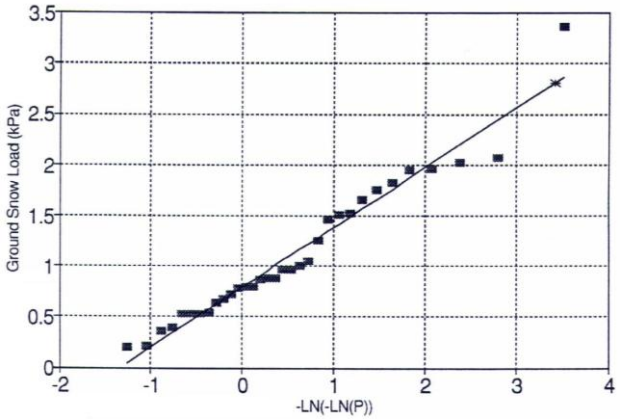

Figure 2 - Fisher-Typett Type 1 extreme values plot ground snow load prediction

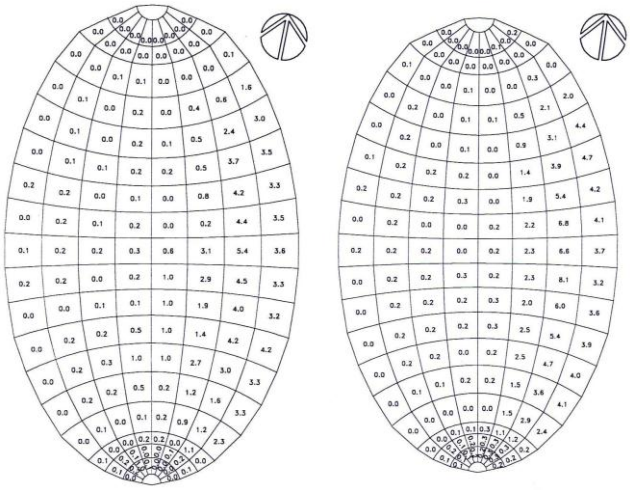

Figure 3 -Comparative analysis of snow loading distribution in function of roof shape (10-13m)

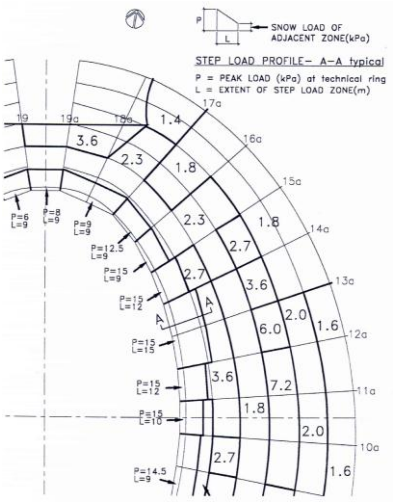

Figure 4 - Sliding and wind snow accumulations step loads

The experimental investigation was carried out by RWDI [3] to provide design snow according to FAE (Finite Area Element) method, representing up to day a state of the art on the matter.

The FAE method uses a combination of wind tunnel tests on a scale model and computer simulation to provide the most accurate assessment possible to estimate 30 year snow loads.

Snow loads depend on many cumulative factors such as, snowfall intensity, redistribution of snow by the wind (speed and direction), geometry of the building and all surroundings affecting wind flow patterns, absorption of rain in the snowpack, and depletion of snow due to melting and subsequent runoff. The current NBCC (National Building Code of Canada) provides minimum design loads for roofs which are based primarily on field observations made on a variety of roofs and on a statistical analysis of ground snow load data. There are, however, numerous situations where the geometry of the roof being studied and the particulars of the site are not well covered by the general provisions of the code. In these situations, a special study, using analytical, computational and model test methods, can be very beneficial since it allows the specific building geometry, site particulars and local climatic factors to all be taken into account. The National Building Code allows these types of studies through its "equivalency" clause and various references to special studies in its commentary.

The model of the three new roof shapes were each constructed at 1:400 scale for the wind tunnel tests. The three model roof designs were each instrumented with 90^o directional surface wind velocity vector sensors covering the surface. On the console roof, an additional 90 sensors were installed. Measurements of the local wind speed and direction, at an equivalent full-scale height of 1 m above the roof surface, were taken for 16 wind directions. The wind speed measurements were then converted to ratios of wind speed at the roof surface to the reference wind speed measured at a height equivalent at full scale to 600 m.

The 30 year ground snow prediction is obtained by interpolation of the data using the Fisher-Typett type I extreme value distribution method (Fig.2), , including both snow and rain (S_s+ S_r), to be 2.8 kPa, which is in agreement with the code value.

Results of structural load cases and local peak loading, not to be considered as acting over the roof simultaneously are shown in Fig. 3-4. The shape of the roof with a sag of more than 12m. gives separation of the air flow and turbulence in the wake increasing considerably the possibility of snow

accumulations. The order of magnitude of the leopardized accumulations in the roof are of 4-15 kN!; local overdimensioning was necessary in order to avoid progressive collapse of the structural system.

2.2 Wind loading-experimental analysis on scale models: rigid structures-quasi static behaviour.

2.2.1 The Cp factors: the Olympiakos Stadium in Athens

Tests have been performed in two distinct phases, the first phase has been devoted to the characterization of the appropriate wind profile in the BLWT, the second one has been dedicated to the identification of the pressure coefficients on the roofing of the new stadium. Because of the great number of pressure taps on the roofing (252), the second phase consisted of three distinct measurement sets.
The stadium is located near to the sea, as a consequence a "sea wind profile" with the parameters listed below and taken from literature and laboratory expertise, seems to be a good approximation of the wind profile in the area (Fig. 5):

profile exponent	$\alpha = 0.15 \div 0.18$ (level ground, with few obstacles, sea),
roughness length	$z_0 = 5 \div 15$ cm (cultivated fields),
integral length scale	$L_U = 50 \div 100$ m.

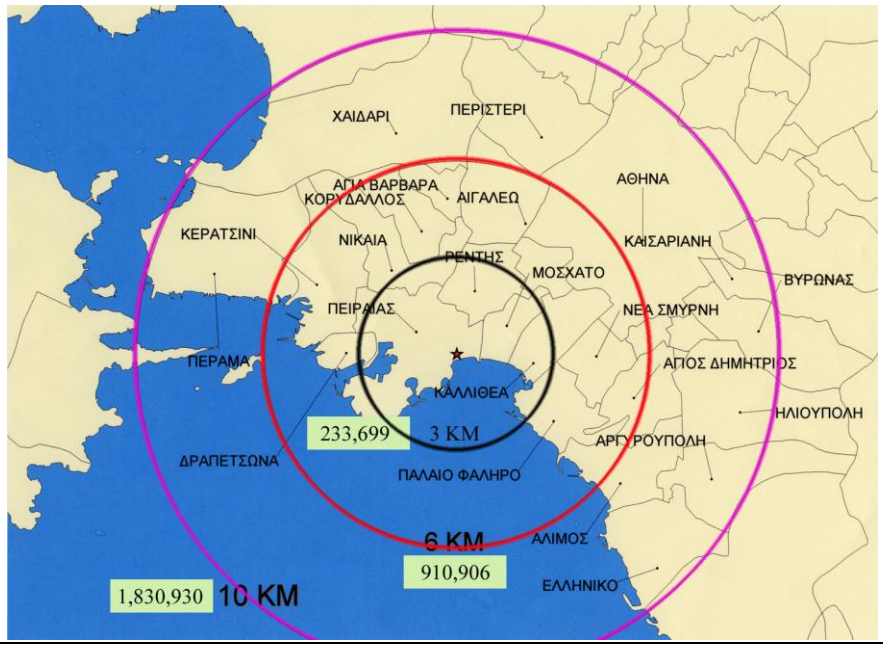

Fig. 5 – Geographic location of the stadium.

In the following paragraph the characteristics of the wind profile actually obtained in the BLWT are examined, and the consistency of the choice in the chosen geometric scale (1:250).

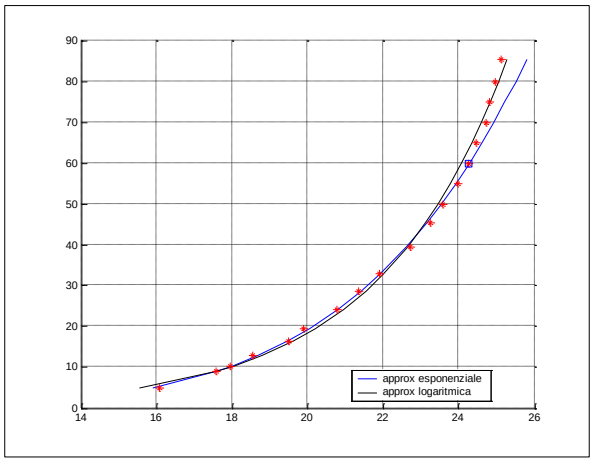

Fig. 6 – Profile of mean wind velocity.

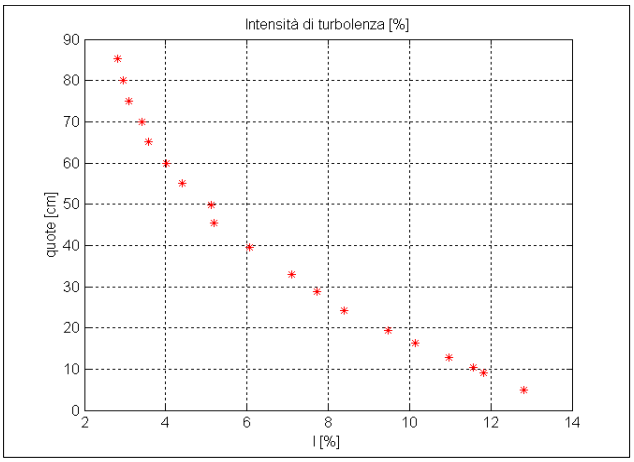

Fig. 7 - Profile of the turbulence intensity

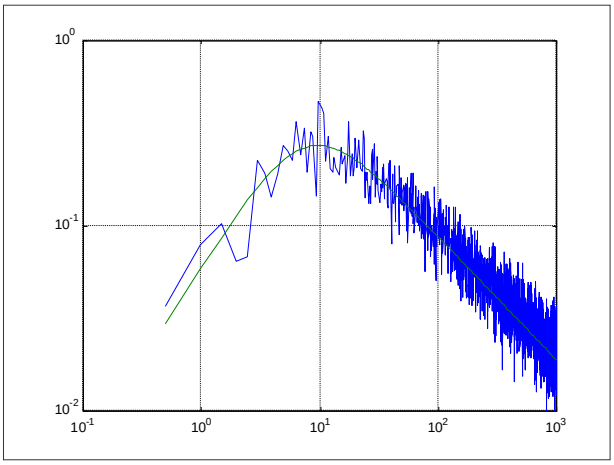

Fig. 8 – Spectral density of the longitudinal component of the wind velocity ("fitting" with Von Karmán spectral density)

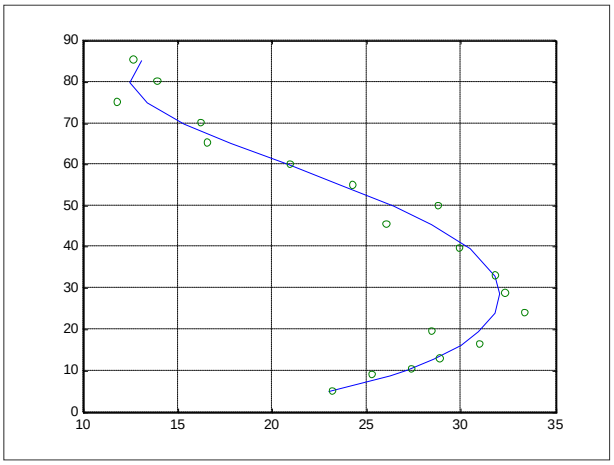

Fig. 9 – Integral length scale at different levels ("fitting" with Von Karmán spectral density).

The model has been made in a geometric scale of 1:250 and includes: the roofing, the stands, all the structures of the stadium, and other private and public buildings not far then 250 m (in full scale) Fig. 10-11 from the centre of the stadium. The geometric scale has been chosen in order to fulfil the similitude laws (Fig. 6-9). In turn the extension of the model around the stadium was dictated by the chosen scale and by the diameter (2 m) of the rotating platform over which the model has been placed in the wind tunnel.

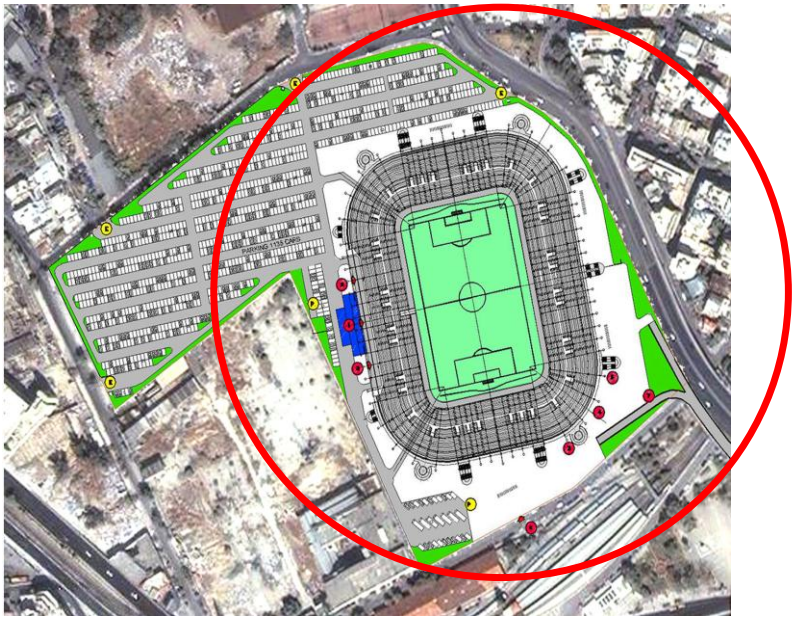

Fig. 10 - Circle which identifies the location of the buildings included in the model.

The roofing has been equipped with 252 pressure taps, of which 126 at the extrados and 126 at the intrados, in order to get the net pressures on the roofing. In the model the roofing of the stadium (Fig.12) has a box structure in order to allow for the settlement of the pressure taps inside. A minimum thickness of about 7 mm has been required for the roofing structure to allow for the insertion of the pneumatic connections. The location of the pressure taps has been chosen to cover the whole roofing surface according to the figure 13, which shows also the influence area of each pressure tap. These areas have been obtained performing a triangulation among the pressure taps and linking together the barycentres of the identified triangles.

Fig. 11 – 3D Renderings

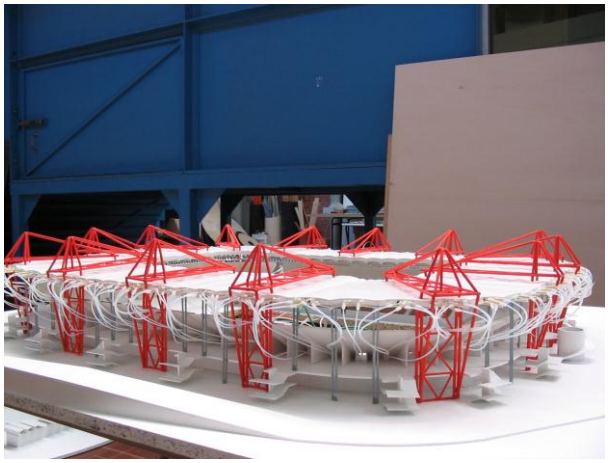

Fig. 12 – Wind tunnel scale model

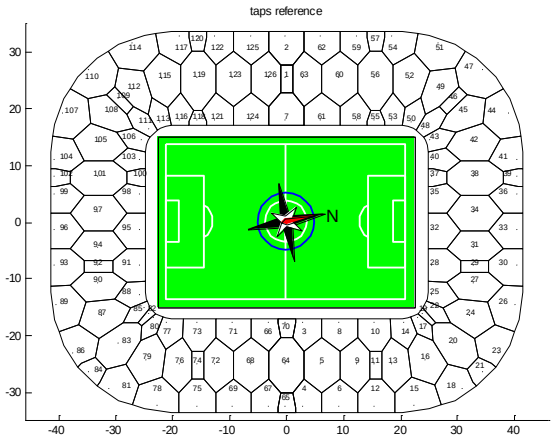

Fig. 13 - Position of the pressure taps (each position corresponds to two pressure taps, one at the extrados and the other at the intrados of the roofing).

In the above figure the positions of the pressure taps are shown together with their influence areas; each position identifies the position of both the tap at the intrados and the tap at the extrados, which lay on the same vertical and are spaced out by the thickness of the box structure of the roofing.
The pressure measurements have been performed using piezoelectric transducers linked to the pressure taps through Teflon pipes (Fig. 14).

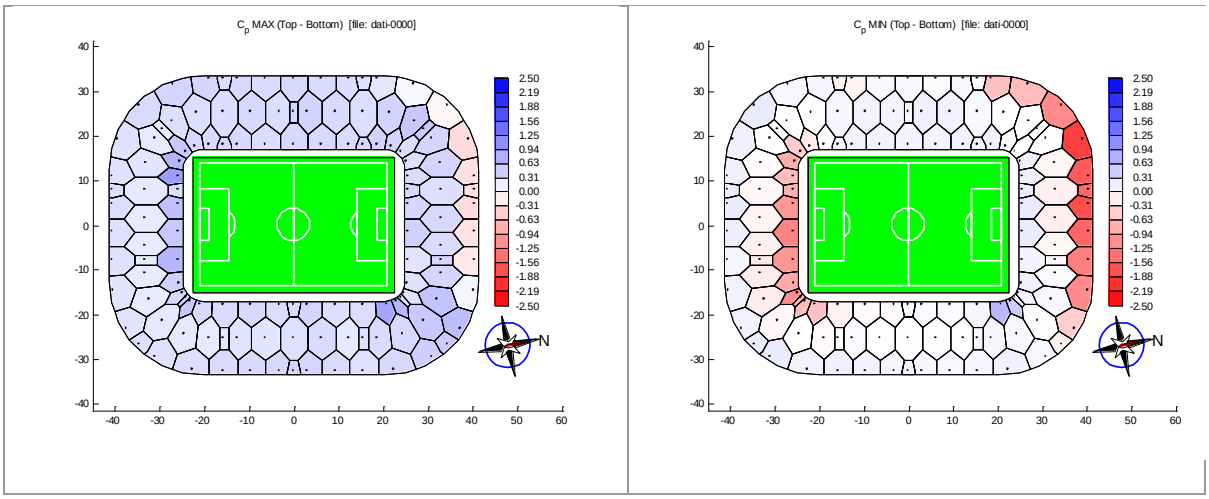

Fig. 14 – Maximum and minimum values of net pressure coefficients (wind direction: 0°).

2.2.2 Measurement and use of load time histories*: The Thessaloniki Olympic sport complex*

The integration of the wind tunnel data into the design process presents significant problems for wide span sub-horizzontal enclosures; in contrast to buildings (high rise buildings) where knowledge of the base moment provides a sound basis for preliminary design, there is not single simple measure for the roof. The study of the Stadium of the Alpes and the Rome stadiums [4-5-6] drew attention to the inability of the measuring system employed to provide data in a form that could readily be based as input to the sophisticated dynamic numerical model developed by the designer and lead to discussion between the designer and the wind tunnel researchers to examine alternate techniques that might be used in future projects [7].

The discussions centered on the use of high speed pressure scanning systems capable of producing essentially simultaneous pressure measurements at some 500 points at rates of perhaps 200 Hz per point. With such a system it would be possible to cover in excess of 200 panels and produce a complete description of the load. Such a system would produce roughly 1 to $2x10^6$ observations for a single wind direction and it is clear that some compression of the data would be required. One possible approach would be to produce a set of load histories, $Q_j(t)$, such that:

$$Q_j(t) = \int_A p(x,y,t)\phi_j(x,y)dA \qquad (1)$$

where:

$p(x,y,t)$ nett load per unit area at position (x,y);

$\phi_j(x,y)$ weighting function.

For a series of pressure taps of the approximation to $\phi_j(t)$ would be:

$$Q_j(t) = \sum_{i=1}^{N} \overline{p}_i(\overline{x}_i,\overline{y}_i,t)A_i\phi_j(\overline{x}_i,\overline{y}_i) \qquad (2)$$

A_i area of ith panel;

p_i	pneumatic average of pressure at the taps in the i[th] panel;
x_i, y_i	geometric centre of the taps on the i[th] panel;
N	number of panels.

The requirements of a system designed to produce the load histories, $\phi_j(t)$, is discussed in the following section.

In collaboration with the Boundary layer wind tunnel laboratory of the University of Western Ontario, a new very practical method to obtain the structural response under the random wind action and small displacements (linear response) has been applied under the name of the "orthogonal decomposition method".

If the weighting functions, $\phi_j(t)$, are chosen as mode shapes then $\phi_j(t)$ is a modal load and its use in conjunction with a dynamic model is clear; either as a set of time histories or a set of modal force spectra and cross-spectra. In the initial stages of a design the roof shape is probably known with reasonable accuracy but mode shapes not so. In such cases it might be appropriate to choose a suitable set of ϕ_j from which modal loads corresponding to shapes ψ_i can be estimated when the design is more advanced. In such a case we can approximate ψ_j as:

$$\psi_j \cong \psi^i_j \sum_i^M a_{ij}\phi_j \tag{3}$$

the values of a_{ij} can be evaluated by minimizing the discrepancy between ψ_j and ψ_j, ie:

$$\frac{\partial}{\partial a_{ij}} \int \left(\psi_j - \sum_i a_{ij}\phi_i \right)^2 dA = 0 \tag{4}$$

$$i = 1, M$$

If the functions ϕ_i are chosen as a set of orthogonal shapes $\int \phi_i \phi_j dA = 0; i \neq j$ then the coefficients are given as

$$a_{ij} = \frac{\int \phi_i \phi_j dA}{\int \phi_i^2 \phi_j dA} \tag{5}$$

For a finite panel sizes the corresponding relationship is:

$$a_{ij} = \frac{\sum_k^N \phi_i(\bar{x}_k, \bar{y}_k)\phi_j(\bar{x}_k, \bar{y}_k)A_k}{\sum_k \phi_i^2(\bar{x}_k, \bar{y}_k)A_k} \tag{6}$$

where:

$$\sum_k^N \phi_i(\bar{x}_k, \bar{y}_k)\phi_j(\bar{x}_k, \bar{y}_k)A_k = 0$$

$$i \neq j$$

The experiment would involve the recording of the local histories $\psi_j(t)$ from which the model time histories could be constructed and the analysis conduced in either the time or frequency domain (Figures 15-18). For the type of structure under consideration resonant effects are small and the response is largely a quasi-static to a spatially varied load. The deflections induced are closely related to the imposed loads and their distribution differs significantly from the Gaussian form [7]. In such a

case the time domain solution, which preserves the extreme value distribution, is to be preferred over a frequency domain approach.

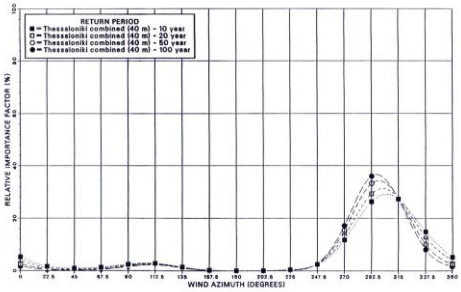

Figure 15 - Relative contribution of Azimuthal Direction to the exceedance probability of various return period wind speeds for Thermi, Thessaloniki, Greece

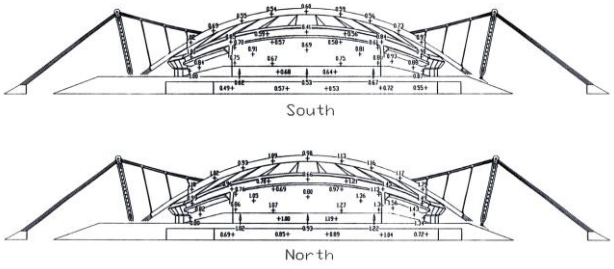

Figure 16 –Taps location

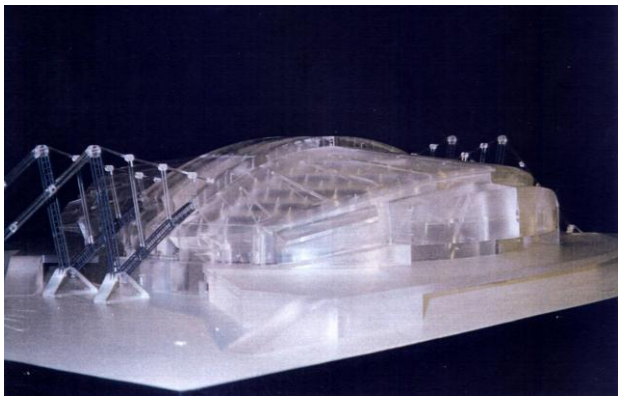

Figure 17 - Views of pressure model

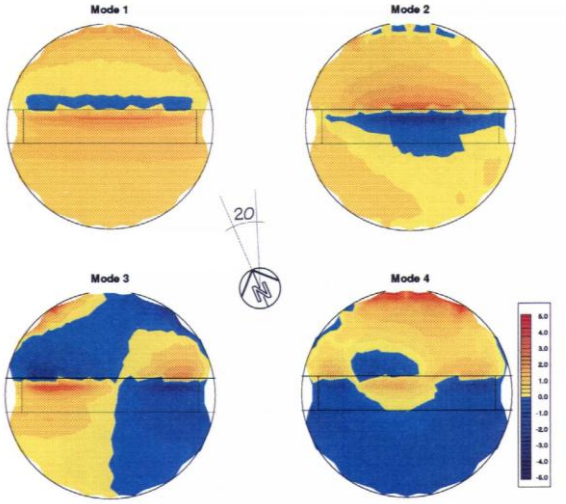

Figure 18 - Orthogonal decomposition: pressure mode shapes

For the seismic analysis a frequency domain approach was adopted. The Kanai-Tajimi PSD was used under the design response spectra prescribed by Eurocode 1; under strong-motion, an acceleration time history was artificially generated according to site and durability characteristics [8].

2.3 Wind loading-experimental analysis on scale models : flexible structures-aerodynamic behaviour: ***The olympic stadium in Rome***

The wind induced response of the cable supported stadium roof was analysed by a non linear model and a field of multicorrelated artificial generated wind loading time histories [6].Wind tunnel tests have been carried out at the BLWT Lab. of UWO on a model of 1:200 Fig. 19 scale determining:
- time histories of the local pressures for every 10° of incoming flow direction;the maximun,minimun and average values of the wind pressure have then been evaluated, as well as the root mean square of its fluctuating part;
- presssure coefficients (maxima,minima and average) for every 10° of incoming direction;

- auto and cross-spectra of the fluctuating pressure (averaged on every single panel).

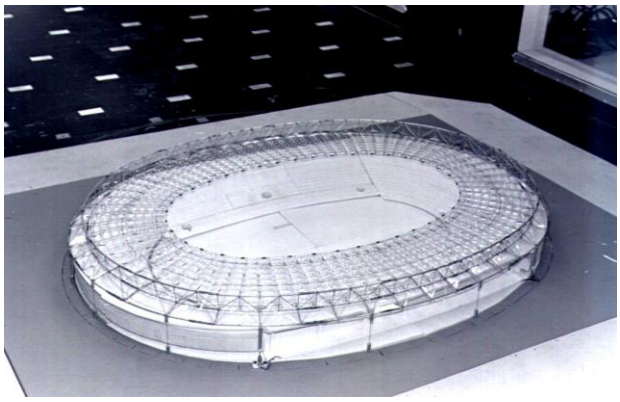

Figure 19 - Aeroelastic model for Rome Olympic Stadium

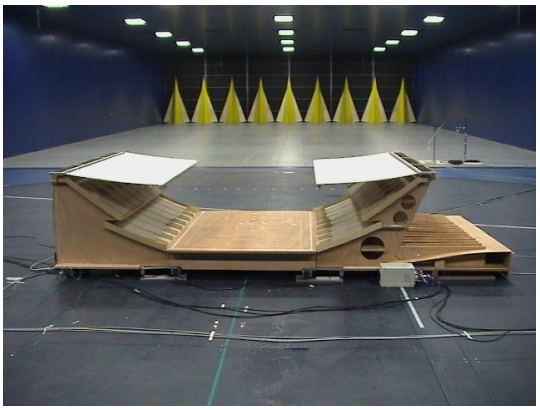

Figure 20 – Aeroelastic model for the Braga Stadium

The aerodynamic behaviour shows a clear shedding phenomenon. The external border of the structure, constituted of the trussed compression ring with triangular section and tubular elements and by the roofing of the upper part of the stands, disturbs the incoming horizontal flow in such a way so that vortex shedding is built up. This causes the roofing structure to be subjected to a set of vortices with a characteristic frequency. This is confirmed by the resulting Power Spectra Density Function of the fluctuating pressures, which shows a peak at about 0.15Hz even if the values rapidly decrease with increasing distance Fig. 21.

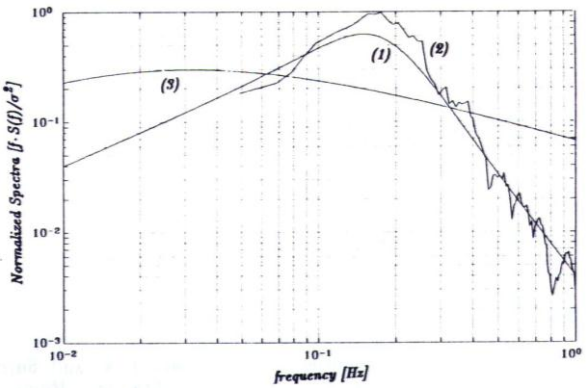

Figure 21 - Target (1), simulated (2) and Kaimal's (3) normalized spectra of wind velocity

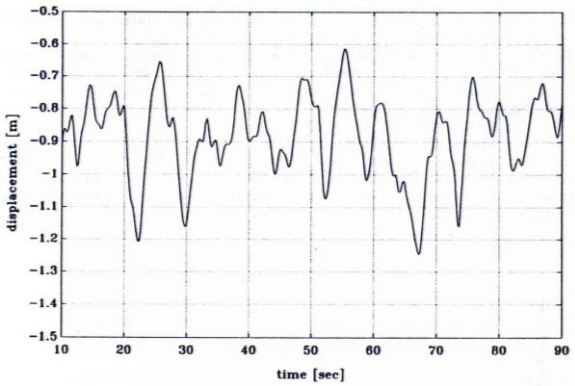

Figure 22 - Time History of the displacement (leeward side at tension ring, run #2)

A fluid-interaction non linear analysis in time domain, made for the checking of La Plata stadium design [9] shows a better agreement between theoretical model and experimental values.

3 RELIABILITY ANALYSIS: *the sensibility analysis regarding the new suspended cable roof of Braga (Portugal)*

3.1 Reliability analysis of the roof structural system. Cable strain parametric sensibility.

Considering that in the basic solution the roof will be covered by a long span structural system with

only uplift gravitational stabilization (Fig. 20) it is essential to proceed to the analysis of the response of the structural system to loading patterns and wind induced oscillations.

The analytical process will be organized in order to be controlled by experimental investigations in reduced and full scale.

The reduced scale experimental analysis on rigid and aeroelastic models are concerned with the determination of the dynamic loading on the roof surface and of the stability of the structural system.

The full scale experimental investigations are addressed to check, by a monitoring program, the validity of the global analysis process.

The uncertainties on the elastic modulus of the cable, geometrical and elastic long term creeping, tolerances of fabrication and erection, differences with design prestress, non uniform distribution of temperature, non linear behaviour, created a sensitive response on the suspended roof hanging from a set of suspended cables. The sensibility analysis showed that the response is sensitive to the standard deviation of the cable strain ($\Delta\varepsilon$) variations. The failure probability is given by the probability that an outcome of the random variables ($\Delta\varepsilon$) belongs to the failure domain D. This probability is expressed by the following integral [10]:

$$P_f = \int_{D_f} f_{\Delta\varepsilon}(\Delta\varepsilon) \cdot d\Delta\varepsilon \tag{7}$$

and the most probable failure mechanism will involve primarily the border cables.

The sensibility analysis was, therefore, extremely important to detect the weak points of the structural system and permits proper local dimensioning to prevent chain failure, as illustrated with the failure simulation of same sensitive cable elements.

The roof is composed by a structural concrete plate sustained by ***n*** prestress cables. In the analysis the roof, the bending moments at ***m*** points will be considered. For a particular load combination, the ***n*** cables have computed strains given by the vector $\boldsymbol{\varepsilon}$. Considering that these effects are represented by the vector of random variables $\boldsymbol{\Delta\varepsilon}$ with mean values $\boldsymbol{\mu}$ and standard variations $\boldsymbol{\sigma}$, the problem is to estimate the probability, P_f, that the generated random bending moments ***M*** will be larger than the plate ultimate resistance moments, $\boldsymbol{M_u}$, at any of the ***m*** points of the structural plates system.

3.2 Roof structural system data

The following probabilistic description was considered for the random variables $\boldsymbol{\Delta\varepsilon}$.

- $\boldsymbol{\mu}$ = Vector of mean values of $\boldsymbol{\Delta\varepsilon = 0}$ (i.e., all possible actions on the cables are considered by the load combination itself).
- $\boldsymbol{\sigma}$ = Vector of standard deviations of $\boldsymbol{\Delta\varepsilon = 0}$. The $\boldsymbol{\sigma}$ values were varied from $0.5\text{x}10^{-3}$ to $0.1\text{x}10^{-3}$ so that the sensibility of the system can be studied. These values were selected to cover the range of failure probabilities of practical significance.
- $\boldsymbol{f_{\Delta\varepsilon}(\Delta\varepsilon)}$ = Probability density function = Normal distribution with parameters $\boldsymbol{\mu}$ and $\boldsymbol{\sigma}$.

3.3 Failure condition

For load case *"i"* the bending moments, M_x, M_y y M_{xy} in the 130 points of the plate can be computed as follow:

$$M_x = M_{Gx_i} + \sum_{j=1}^{34} A_{x_{i,j}}.\Delta\varepsilon_j \qquad M_y = M_{Gy_i} + \sum_{j=1}^{34} A_{y_{i,j}}.\Delta\varepsilon_j \qquad M_{xy} = M_{Gxy_i} + \sum_{j=1}^{34} A_{xy_{i,j}}.\Delta\varepsilon_j \tag{8}$$

Considering the bending moments in each direction, the failure functions at each point of the plate ($1 \le r \le 130$), $G_r(\boldsymbol{\Delta\varepsilon})$, are the following hyperplanes,

$$M_{Upx} - (M_{Gx_i} + \sum_{j=1}^{34} A_{x_{i,j}}.\Delta\varepsilon_j) < 0 \qquad M_{Upy} - (M_{Gy_i} + \sum_{j=1}^{34} A_{y_{i,j}}.\Delta\varepsilon_j) < 0 \tag{9}$$

$$M_{Unx} - Abs(M_{Gx_i} + \sum_{j=1}^{34} A_{x_{i,j}}.\Delta\varepsilon_j) < 0 \qquad M_{Uny} - Abs(M_{Gy_i} + \sum_{j=1}^{34} A_{y_{i,j}}.\Delta\varepsilon_j) < 0 \tag{10}$$

$$M_{Uxy} - Abs(M_{Gxy_i} + \sum_{j=1}^{34} A_{xy_{i,j}}.\Delta\varepsilon_j) < 0 \tag{11}$$

where $G_r \le 0$ is failure and M_{Uxy} is computed from the Johanssen Theory as the smallest of the following expressions

$$M_{Uxy} = (M_{Upx} + M_{Upy})/2 \qquad M_{Uxy} = (M_{Unx} + M_{Uny})/2 \tag{12}$$

In these formulas, M_{Upx}, M_{Upy}, M_{Unx}, M_{Uny} and M_{Uxy} are considered always positive.
The failure condition is obtained when failure is reached at any point of the plate, i.e., the structural failure can be defined as

$$(G_1 \le 0) \cup (G_2 \le 0) \cup \_ \cup (G_{130} \le 0) \tag{13}$$

3.4 Solution method

Since a closed form solution is not possible for the integral in (7) the failure domain defined by equations above, Montecarlo Simulation must be used. By Montecarlo Simulation, the failure probability is obtained by computing $\boldsymbol{G_r(\Delta\varepsilon)}$ for several values of $\boldsymbol{\Delta\varepsilon}$ generated with normal distribution. An approximation to the failure probability is obtained by counting the number of times that $\boldsymbol{\Delta\varepsilon}$ belong to the $\boldsymbol{D_f}$ with respect to the total number of simulations. For small failure probabilities, however, direct application of Montecarlo Simulation is not possible because of the large number of needed iterations to get enough accuracy. To avoid this problem, the Orientated Simulation Method was used in this report. A complete description of the method can be found in the paper [10].

3.5 Results and conclusions

All the load cases were analysed and the following preliminary conclusions are described as follows.
In order to identify the most dangerous load case the minimum reliability index β for each load cases were calculated for a standard deviation σ =0.5 x 10^{-3} for $\boldsymbol{\Delta\varepsilon}$ of all cables. The following table (Table 2) summarizes the index β (computed with σ =0.5 x 10^{-3}).

Table of

Load Case	Beta	Phi(-Beta)
1	5.8739	2.14E-09
2	5.7957	3.42E-09
3	5.9555	1.31E-09
4	5.5733	1.26E-08
5	4.1218	1.87E-05
6	4.8436	6.41E-07
7	1.6658	4.79E-02
8	5.7281	5.11E-09
9	5.5396	1.53E-08
10	2.6269	4.31E-03
11	2.3812	8.63E-03
12	4.3046	8.37E-06
13	4.3045	8.37E-06
14	5.8201	2.96E-09
15	5.7479	4.55E-09
16	5.8415	2.61E-09

The load cases 7, 9 and 10 have the lowers β, i.e., the higher failure probability, and therefore they are the critical load condition. Particularly critical is the load case 7.

3.5 Failure probability and sensibility analysis

The figure 23, shows the failure probability for load combination 7 as a function of the standard deviation, σ, of the cable strain variations, $\Delta\varepsilon$.

a. The problem is extremely sensitive to the standard deviation, σ, of the cable strain variations, Δε. For example for load case 7, if σ is increased from $2x10^{-4}$ to $3x10^{-4}$, Pf is increased from $2x10^{-5}$ to $480x10^{-5}$.
b. Cable standard deviation, σ, should be maintained below $2x10^{-4}$ for the designed ultimate bending moment.
c. Larger cable standard deviation, σ, could be allowed increased the slab reinforcement along x-direction in the critical roof zone.

The figure 24, shows the most probable values of Δε ($x10^{-3}$) in each cable at failure for load combination 7.

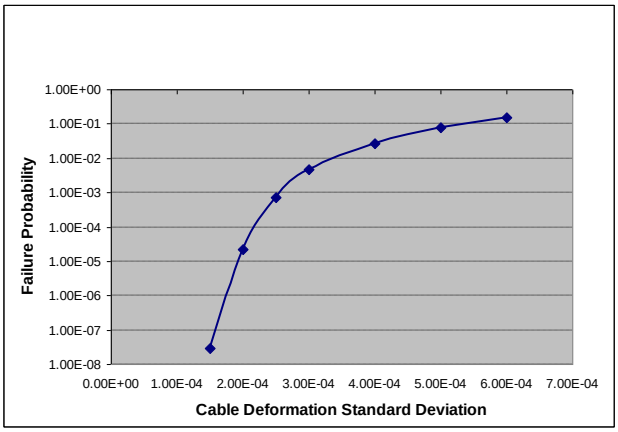

Figure 23 – Failure probability in function of cable deformation standard deviation

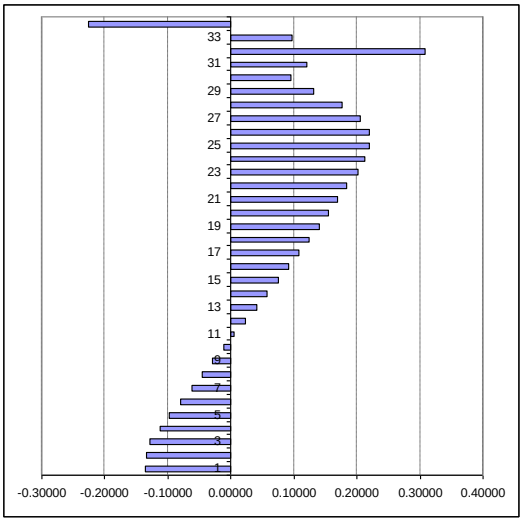

Figure 24 – Most probable Δε meach cable at failure for load comb. 7

The following comments can be done.

a. The most probable values of Δε are practically independent of the standard deviation σ. In other words, the configuration at failure is constant. This configuration is reached with more probability as the standard deviation of Δε increases.
b. The most probable configuration at failure is mainly due to variations in the strains of cables 32 and 34. Since elongations of cables can be computed as ΔL=L Δε, the elongation at failure of cables 32 and 34 are approximately ΔL_{32}=210m x (-0.2x10-3) = 4.2 cm and ΔL_{34}= 210m x (0.3 x10-3) = 6.3 cm.

4 MONITORING

The roof structures of the Torino Stadium have been built in 1990. According to the quality control and maintenance program, the in service subsequent performance of the structure has been controlled by site inspection, experimental measurement and spot monitoring of representative structural parameters. The anchorage forces in the cable stays have been controlled during 1992 and considerable differences in average and peak values of pre-stressing have been observed between experimental and expected theoretical values. The authors proceeded, with a computer simulation of the actual observed anchorage force values, to determine a new pre-stressing sequence in order to fit the original design cable force. Actually the structure is under normal monitoring observation according to a special maintenance program.

4.1 Displacement and force control.

The first tensional controlling operations were performed on the cable anchorage forces in 08.05.1992. The geometrical control of the central ring was performed during and after the completion of the operations, dated 13.05.1992. On the 19.05.1992 the designers were requested to conceive an intervention plan to eliminate the detected errors related to the intensity and distribution of the state of initial stress.

Therefore, on the 3.08.1992, it was presented a proposal related to a theoretical simulation of the experimentally observed stressing state and to the definition of a correct new pre-stressing. The comparative analysis between the results, referred to the actual service state anchorage forces (whose permanent loads were updated according to the final consumptive analysis) and the experimental data, revealed average and peak values' differences bigger than the allowable ones. The average prestressing level is reduced of 30%, with peak differences of 40-50% (Fig. 25-26).

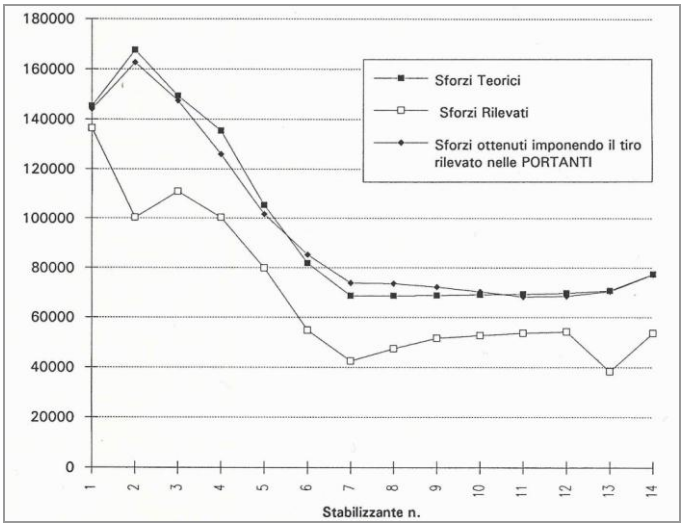

Figure 25 Stabilizing cable. Anchorage forces. Computed actual values. Measured values. Restored values.

4.2 Interpretation of results.

In order to have a better scenario of the pre-stressing level and distribution, a new control of all anchorage forces under uniform temperature condition (night-time) had been produced. The results confirmed the spot control measurements. Considering the main characteristics of the structural typology adopted or the stadium the variation of the pre-stressing state can be related principally to:

- non uniform temperature variation;
- elastic an anelastic foundations' settlements and soil interactions;
- random errors in cutting or marking the cables;
- geometrical, elastic or anelastic short and long term creeping of cables;
- errors in pre-stressing procedure.

The theoretical simulations, which include the compsuntive updating of the permanent loads, provide to the eliminations of the uncertainties related to the loading variation's influence. The soil conditions and measurements of settlements during 4 years permit to remove any consideration of influence of soil interaction in variation of pre-stressing level. Measurements taken during night-time show no influence for temperature variations.

Considering that peak values are random distributed it is also possible to disregard the influence of errors in cutting and marking of cables, normally respecting the symmetry of construction. The logical answer, therefore, confirmed by a parallel experience on the structural system of the Olympic Stadium in Rome, is that the variation noted in pre-stressing level of the system can be related to a combinations of creeping and to uncertainties concerning the pre-stressing procedure.

"Geometrical" equivalent creeping of spiral strands is supposed to be removed by 50% breaking load shop prestressing cycles. Many cable structures showed creeping in short and long term. Creeping of cables is not well documented in technical literature. Some fabricators give 3‰ as "possible values" of anelastic creeping which imply the impossibility to guarantee any value of E-modules (3‰ of E imply a variation of 500 N/mm^2 !).

Measurements of the geometry of the central ring show a separation between expected theoretical and measured values, but the experimental Z-configuration of the ring had only small variations in time during 3-year observations.

The consequence of the above mentioned observations is that the changements observed in the pre-stressing state must be related principally to the procedure of pre-stressing under high gradient of daily temperature variations. The tensostructure was prestressed by an iterative "step by step" sequence. The number of steps have to be determined in function of the characteristics of the structural system as the parametric sensibility, the correlation degree between incremental values and the verification of the level of the transitory sequential overstressing. The reliability of the process is increased by the number of iterations, allowing to calibrate and automatically control the pre-stressing according with a predictor-corrector techniques.
As a matter of fact, probably in order to reduce the time needed for the operation, it was decided to make the pretensioning in just one step. This choice allowed the minimization of the reliability of the process even though the geometric, mechanic, thermical variations along with those related to the mathematical modeling of the pretensioning simulation could contribute to increase, effectively, the varying between the project's values and the ones related to the expected forces, actually induced. The designers recommended the functional restore of the in service state by bringing the pre-stressing values back to the average expected ones.

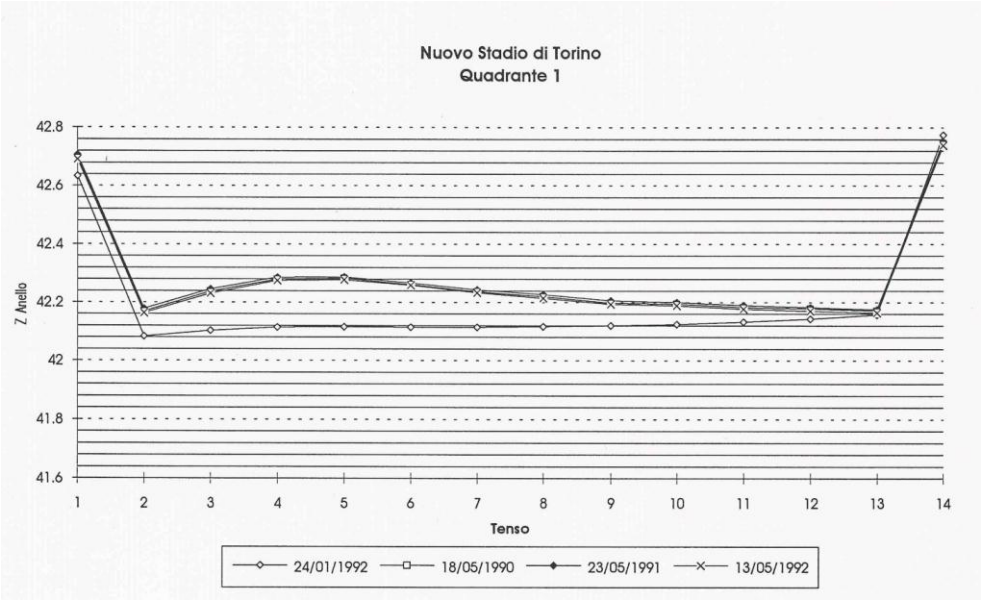

Figure 26 Z coordinate of the inner ring according to experimental measurement.

4.3 Measurements and monitoring.

A special monitoring program was adopted during transitory time in order to control the displacements of some points of the roof.

Before and after the pre-stressing procedure a dynamic load was applied to the structure and, with the use of a special accelerometer giving efficient possibility to integrate accelerations in range of low frequencies (< 10-1 Hz) , power spectral densities of response could be plotted. With the frequencies and associated mode shapes it was possible to observe the increase of geometrical stiffness of the structural system by the new pre-stressing level. Accelerations and displacements, before and after prestressing, are shown in Table 3.

	Acceleration m/sec^2	
	Before	After
A3	0.93 - 1.19	0.86 - 0.96
A4	0.50 - 1.00	0.32 - 0.44
	Displacements mm	
	Before	After
A3	7.8 - 10.0	6.8 - 7.5
A4	6.8 - 9.2	5.2 - 7.1

Table 3 Accelerations and displacements under dynamic load before and after pre-stressing.

CONCLUSIONS

It has been noted the influence of knowledge base on conceptual design in removing gross human intervention errors from initial design statements.

Design assisted by experimental investigation is a useful integration of the design process of wide span structures.

Sensibility analysis is an extremely powerful tool to determine the influence of parametric design uncertainties for unusual long span structural systems.

REFERENCES

[1] R.E. Melchers: Structural reliability, Elley Horwood ltd. 1987.

[2] Structural Design Of Retractable Roof Structures, IASS working group n°16, WIT Press, 2000

[3] RWDI: Roof snow loading study-roof re-design Olympic Stadium Montreal, Quebec. Report 93-187F-15, 1993.

[4] M. Majowiecki: Observations on theoretical and experimental investigations on lightweight wide span coverings, International Association for Wind Engineering, ANIV, 1990.

[5] B.J. Vickery, M. Majowiecki: Wind induced response of a cable supported stadium roof. Journal of Wind Enginerring and Industrial Aerodynamics, 1992, pp. 1447-1458,

[6] B.J. Vickery: Wind loads on the Olympic Stadium - orthogonal decomposition and dynamic (resonant) effects. BLWT-SS28A, 1993.

[7] M. Majowiecki: Snow and wind experimental analysis in the design of long span sub-horizontal structures, J. Wind Eng. Ind. Aerodynamics, 1998.

[8] M. Majowiecki, F. Zoulas, J. Ermopoulos: "The new sport centre in Thermi Thessaloniki": conceptual design of the structural steel system, IASS Congress Madrid, september 1999.

[9] M. Lazzari, M. Majowiecki, A. Saetta, R. Vitaliani : "Analisi dinamica non lineare di sistemi strutturali leggeri sub-horizzontali soggetti all'azione del vento",5° Convegno Nazionale di Ingegneria del vento, ANIV; Perugia 1998.

[10] A.G. Puppo, R.D. Bertero, : "Evaluation of Probabilities using Orientated Simulation", Journal of Structural Engineering, ASCE, Vol. 118, No. 6, June 1992.